

Effects of the Preheating Temperature on the Crystal Structure and Texture of Martensitic Stainless Steel

Tri Hardi Priyanto*, Rifai Muslih, Herry Mugirahardjo, Bharoto, Andon Insani, and Muzzakiy

Center for Science and Technology of Advanced Materials, BATAN, Kawasan Puspiptek, Serpong, Tangerang 15314, Indonesia

*e-mail: thardi@batan.go.id

Abstract

Theoretically, the preheating temperature refers to the start martensite temperature (M_s), and the martensite transformation can be considered as the conservation of the invariant habit-plane in the lattice structure. The habit-plane is the interface plane between austenite and martensite as measured on a macroscopic scale. From the calculation, $M_s = 252$ °C. The martensite formation can be affected by temperature or stress treatment. In this experiment, temperature treatment was conducted. The sample was treated at 250 °C \pm 10 °C. Before and after the pre-heat treatment, the sample was characterized using the neutron diffraction method. BATAN's Texture Diffractometer (DN2) with a neutron wavelength of 1.2799 Å was used to characterize the sample. Analysis of the crystal structure showed that there are three phases before the preheating. The lattice parameters (a) obtained were as follows: for the α -phase, $a = 2.8501 \pm 0.0004$ Å; for the α' -phase, $a = b = 2.517 \pm 0.003$ Å, and $c = 3.581 \pm 0.002$ Å; for the γ -phase, $a = 3.5884 \pm 0.0004$ Å, $R_{wp} = 17.94\%$, and $\sigma = 1.33$. After preheating, only the γ -phase appears with $a = 3.5830 \pm 0.0005$ Å, $R_{wp} = 26.03\%$, and $\sigma = 1.17$. The orientation distribution function is modeled by the sample symmetrization model based on triclinic to orthorhombic sample symmetry. It shows that, before being preheated, the γ -phase has $\{100\} \langle 001 \rangle$ with texture index (F^2) between 0.701 m.r.d. to 3.650 m.r.d., the α -phase has a texture index between 0.923 m.r.d. to 1.768 m.r.d., and the α' -phase has a texture index between 0.910 m.r.d. to 1.949 m.r.d. After being preheated, the γ -phase also has $\{100\} \langle 001 \rangle$ with a texture index between 0.846 m.r.d. to 3.706 m.r.d. It can be concluded, that because of the high preheating temperature, a phase change from martensite to austenite occurred that allowed the sample to be welded easily. After preheating, the γ -phase has the same cubic type orientation $\{100\} \langle 001 \rangle$, and the texture index is nearly the same as that before preheating, with not martensite present.

Abstrak

Pengaruh Suhu Pemanasan-Awal pada Struktur Kristal dan Tekstur Baja Tahan Karat Martensitik. Secara teoritis, suhu pemanasan awal mengacu pada suhu martensit awal (M_s), dan transformasi martensit dapat dianggap sebagai konservasi dari *habit-plane* invarian dalam struktur kisi. *Habit-plane* adalah bidang antarmuka antara austenit dan martensit yang diukur pada skala makroskopik. Dari perhitungan, $M_s = 252$ °C. Pembentukan martensit dapat dipengaruhi oleh suhu atau perlakuan tekanan. Dalam percobaan ini, perlakuan suhu dilakukan. Sampel diperlakukan pada 250 °C \pm 10 °C. Sebelum dan sesudah perlakuan pemanasan-awal, sampel dikarakterisasi menggunakan metode difraksi neutron. Difraktometer Tekstur BATAN (DN2) dengan panjang gelombang neutron $1,2799$ Å digunakan untuk mengkarakterisasi sampel. Analisis struktur kristal menunjukkan bahwa ada tiga fase sebelum pemanasan awal. Parameter kisi (a) yang diperoleh adalah sebagai berikut: untuk fasa- α , $a = 2,8501 \pm 0,0004$ Å; untuk fasa- α' , $a = b = 2,517 \pm 0,003$ Å, dan $c = 3,581 \pm 0,002$ Å; untuk fasa- γ , $a = 3,5884 \pm 0,0004$ Å, $R_{wp} = 17,94\%$, dan $\sigma = 1,33$. Setelah pemanasan awal, hanya *fase appears* yang muncul dengan $a = 3,5830 \pm 0,0005$ Å, $R_{wp} = 26,03\%$, dan $\sigma = 1,17$. Fungsi distribusi orientasi dimodelkan oleh model simetrization sampel berdasarkan sample simetri triclinic ke orthorhombic yang menunjukkan bahwa sebelum dipanaskan fasa memiliki orientasi $\{100\} \langle 001 \rangle$ dengan indeks tekstur (F^2) antara 0,701 m.r.d. hingga 3,650 m.r.d., fasa- α memiliki indeks tekstur antara 0,923 m.r.d. sampai 1,768 m.r.d., dan fase α' memiliki indeks tekstur antara 0,910 m.r.d. sampai 1,949 m.r.d. Setelah dipanaskan, fasa- γ juga memiliki orientasi kubik $\{100\} \langle 001 \rangle$ dengan indeks tekstur antara 0,846 m.r.d. sampai 3,706 m.r.d. Dapat disimpulkan, bahwa karena suhu pemanasan-awal yang tinggi, perubahan fasa dari martensit menjadi austenit terjadi, yang memungkinkan sampel dilas dengan mudah. Setelah pemanasan awal, fasa- γ memiliki orientasi jenis kubik yang sama, yaitu $\{100\} \langle 001 \rangle$, dan indeks tekstur hampir sama seperti sebelum pemanasan awal, dengan tidak hadirnya martensit.

Keywords: martensite, ferrite, austenite, preheating temperature, texture, neutron diffraction

1. Introduction

Stainless steels are known because of their excellent corrosion resistance, moderate hardness, and good wear resistance. Stainless steels are defined as iron base alloys that contain at least 10.5% chromium. The thin but dense chromium oxide film that forms on the surface of stainless steel provides corrosion resistance and prevents further oxidation [1]. The martensitic grades of stainless steel are the smallest groups of stainless steel. To improve the strength and hardenability of the martensitic grades, they have higher carbon content compared to the other grades. The martensitic stainless steels are widely used in many industries because of their excellent mechanical properties and sufficient corrosion resistance. These steels are typically used in a wide range of applications, e.g., nuclear power plants, steam generators, mixer blades, pressure vessels, turbine blades, surgical tools, and instrument manufacturing [2]. A variety of experiments using martensite stainless steel have been conducted, for example AISI 410 were conventionally heat treated in diverse quenching environments to obtain three different microstructures: fine ferrite, fine and coarse martensite [3]. Despite these studies, a question remains: Why is preheating sometimes required before welding? Preheating the steel to be welded slows the cooling rate in the weld area. This reduced cooling rate may be necessary to avoid cracking of the weld metal or the heat affected zone. The need for preheating increases with steel thickness, weld restraint, the carbon/alloy content of the steel, and the diffusible hydrogen of the weld metal. Preheating is commonly applied using fuel gas torches or electrical resistance heaters. The purposes of the preheating treatment are to reduce the risk of hydrogen cracking, to reduce the hardness of the weld heat affected zone, and to reduce shrinkage stresses during cooling and improve the distribution of the residual stresses.

The carburized layer growth of AISI 420 steel as a function of processing temperature and time was studied to understand its physical phenomenon [4]. The effect of austenitizing on the microstructure and hardness of two martensitic stainless steels was examined to ensure a martensitic structure with minimal retained austenite [5]. Another experiment performed was implantation of nitrogen ions at various energies and doses into the surface of AISI 420 martensitic stainless steel [6]. The main problem related with the welding of low carbon 12% Cr stainless steels is its hydrogen induced cracking susceptibility. Thus, it is common practice to perform welding using two alternative approaches; preheating the welded parts and using similar filler material or using an austenitic stainless steel filler metal without preheating. The effect of preheating temperature plays an important role in the welding of martensitic stainless steels. Martensite is classified into three types of crystal structures: BCC (α -phase), BCT (α' -phase), and HCP (ϵ -phase) [7]. The preheating temperature can affect the

change of crystal structure from martensite to austenite (γ -phase) [8]. In contrast, a pre-heating stage has a negligible impact on the microstructure and texture of cold-rolled low carbon steel [9].

Theoretically, the preheating temperature refers to the start martensite temperature (M_s) and the martensite transformation can be viewed as the conservation of the invariant habit-plane in the lattice structure; the start martensite temperature is calculated as described in reference [10]. The results indicate how the thermal cycle, different hydrogen levels and hydrogen trapping sites affect the mechanical properties [11]. In the characterization of stainless steel materials, diffraction methods, such as neutron diffraction methods, are used to characterize the physical and mechanical properties, such as the density and substructure of dislocations during tempering [12], strain-induced martensitic transformation [13], and bulk phase transformation [14]. Characterization using the neutron scattering technique is still rarely performed in Indonesia, especially research of material texture by using diffraction method. Characterization of textures inside of the test material (known as bulk texture) is possible using neutron diffraction.

This paper discusses the influence of preheating on base metal martensitic stainless steel and its effect on the direction of crystal orientation (texture).

2. Experimental Methods

Material. Two samples of SS420 martensite stainless steel were characterized: one was taken before preheating, named sample A, and the other was taken after preheating, named sample B. The dimensions of each sample were 10 mm \times 10 mm \times 10 mm. Each sample was cut from a stainless steel plate using a wire cutter.

Preheating temperature. Preheating involves heating of an entire region to a specific desired temperature (preheat temperature). Preheating is the process applied to raise the temperature of the parent steel before welding. Preheating is used for the following main reasons: 1) to reduce the cooling rate of the weld and the base material, resulting in a softer weld metal and heat affected zone microstructures with a greater resistance to hydrogen cracking during fabrication; 2) the lower cool rate encourages hydrogen diffusion from the weld area by extending the time period over which it is at elevated temperature (particularly the time at temperatures above approximately 100 °C) at which temperatures hydrogen diffusion rates are significantly higher than at ambient temperature; the reduction in hydrogen reduces the risk of cracking, and different hydrogen levels and hydrogen trapping sites affect the mechanical properties [11].

Neutron diffraction. The neutron diffraction method has advantages over the x-ray diffraction method because

neutrons are uncharged (neutral), thereby allowing for sufficient penetrating power when interacting with matter and because neutrons with magnetic spins are particularly useful for characterizing magnetic materials. Neutrons are generated from GA Siwabessy reactors that operate at 15 MW power, and DN2 texture diffractometers are used for texture data retrieval. Figure 1(a) shows the textural diffraction and Figure 1(b) shows welded martensite stainless steel sample used in the characterization tests.

The samples were characterized using a neutron texture diffractometer DN2. A neutron wavelength of 1.7999 Å was used to obtain the neutron diffraction data. The neutrons were generated by a beam tube S5 of GA Siwabessy reactor.

Before each sample was characterized using the neutron diffraction method, the chemical composition was determined precisely, and the sample before preheating was analyzed using Arc Spark Spectroscopy. Spark or arc atomic emission spectroscopy was used for the analysis of the metallic elements in the solid samples. A sample of each solid was commonly ground up and destroyed during analysis. An electric arc or spark was passed through the sample, heating it to a high temperature to excite the atoms within it. The excited analyte atoms emit light at characteristic wavelengths that can be dispersed with a monochromator and detected. Elemental analysis using spark sources with controlled discharges can be considered as quantitative.

Calculation of the preheating temperature. Determination of the optimum preheating temperature for all martensitic steels (1) is important. When a martensitic steel piece is to be welded, the heated steel contains higher levels of alloying elements. The calculation of the martensite starts temperature (M_s) based on Andrew's empirical formula is not appropriate [15]. Another equation recommended for determining the M_s temperature of martensitic creep-resistant steels is as follows (concentrations are in wt-%) [10]:

$$M_s = 454 - 210C + 4.2/C - 27.Ni - 7.8.Mn - 9.5 * (Cr + Mo + V + W + 1.5 - Si) - 21.Cu \quad (1)$$



Figure 1. (a) Texture Diffractometer DN2 and (b) Welded Martensite Stainless Steel Sample

3. Results and Discussion

Chemical composition analysis and calculation of the preheating temperature. Testing with Spark emission spectroscopy is conducted at three points, and the value taken is the average value. Generally, martensitic stainless steels contain 11 to 18% Cr, up to 1.20% C, small amounts of Mn and Ni, and (sometimes) Mo. From the Spark emission spectroscopy result, the main chemical composition of the sample tested is similar to that of the factory specifications. Several elements observed from the sample test using Spark emission spectroscopy can be categorized as impurities. Table 1 shows the results of the composition test of materials using Spark emission spectroscopy. To improve the strength and hardenability of the martensitic grades, the carbon content is increased compared to that of other grades, and nitrogen is sometimes added to further improve the strength. These grades contain no (or quite small amounts) of nickel, and molybdenum is seldom added. By adding some nickel and reducing the carbon content, the rather poor weldability of martensitic grades can be improved. Sometimes sulfur is added to improve the machinability.

From calculation of the preheating temperature based on the composition shown in Table 1 and equation (1), the martensitic start temperature, $M_s = 252$ °C. Based on the temperature calculation, the sample test was heated to the temperature of approximately 250 °C \pm 10 °C.

Neutron diffraction analysis: Crystal structure analysis. From the neutron diffraction data refinement, sample A has three phases: ferrite (α -phase), martensite (α' -phase), and austenite (γ -phase). MAUD (Materials Diffraction Using Diffraction) software was used to refine the lattice parameters. From the data refinement, sample A has the lattice parameters of the α -phase with Im-3m space group of $a = b = c = 2.8499$ Å \pm 0.0004 Å. The lattice parameters of the γ -phase with space group Fm3m are $a = b = c = 3.517$ Å \pm 0.0004 Å, and the α' -phase with space group I4/mmm has lattice parameters of $a = b = 2.517$ Å \pm 0.004 Å, $c = 3.581$ \pm 0.002 Å. The diffraction pattern of these phases are shown in Figure 2 and Table 2. The reliability factors of $R_{wp} = 17.95\%$ & $R_{exp} = 14.71\%$ and $\sigma = 1.22$ are obtained.

Table 1. Chemical Composition (weight %) of Martensitic Stainless Steel Obtain from Spark Emission Spectroscopy

C	Si	Mn	P
0.10	0.37	1.06	0.05
S	Cr	Ni	Mo
0.003	13.7	2.35	0.0024
Al	Co	Cu	Nb
0.01	0.155	0.826	0.388
Ti	V	W	Pb
0.0031	0.115	0.04	0.015

The transformation of martensite into austenite occurs as a result of the heating process. Martensite transformation can be visualized as a shear of the parent phase into the product phase that conserves an invariant habit-plane in the lattice structure. This transformation is diffusionless, i.e., the chemical composition of the austenite (parent phase) and martensite (product phase) are identical, with no redistribution or exchange of atoms. This transformation is accomplished by shifting

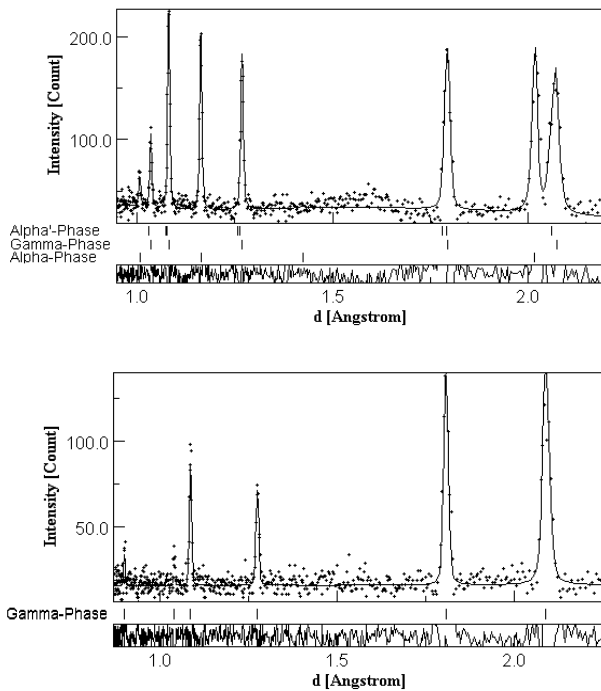


Figure 2. Diffraction Pattern of MSS (a) Before and (b) After the Preheating Process.

Table 3. Phase Types, Bragg Peaks, and Lattice Parameters of the Sample Test

Phase	Bragg peaks	Lattice parameters (Å)
Before preheating		
γ -Fe	(111), (200), (220), (311), (222)	$a = b = c = 3.5872 \pm 0.0004$, $\alpha = \beta = \gamma = 90^\circ$
α -Fe	(110), (200), (211), (220)	$a = b = c = 2.8499 \pm 0.0004$, $\alpha = \beta = \gamma = 90^\circ$
α' -Fe	(101), (002), (110), (112), (200), (103), (211), (202)	$a = b = 2.517 \pm 0.004$, $c = 3.581 \pm 0.002$, $\alpha = \beta = \gamma = 90^\circ$
After preheating		
γ -Fe	(111), (200), (220), (311), (222), (400)	$a = b = c = 3.5929 \pm 0.0004$, $\alpha = \beta = \gamma = 90^\circ$

the atoms simultaneously at a distance of no more than the distance between atoms (lattice spacing).

These movements are small, usually less than the inter-atomic distances, and the atoms maintain their relative disposition. However, this movement of atoms can give rise to three different crystal structures of martensite: body-centered tetragonal structure (bct), defined as α' -martensite; body-centered cubic (bcc), defined as α -martensite; and hexagonal close-packing (hcp), defined as ϵ -martensite [7]. In sample B, only the austenite phase appears, and the lattice parameter 3.5929 ± 0.0004 Å, $\alpha = \beta = \gamma = 90^\circ$, was obtained from crystal structure analysis. The reliability factors were found to be $R_{wp} = 26.03\%$ & $R_{exp} = 22.19\%$, and the goodness of fit was found to be $\sigma = 1.17$. The diffraction peak analysis showed that peak (200) in the α -phase was damped. This result is consistent with a result reported in reference [2]. This result corresponds to "Bain strain" where contraction occurs along the $[0\ 0\ 1]$ γ axis and a uniform expansion occurs on the $(0\ 0\ 1)$ γ plane [8].

Texture analysis: Texture before preheating. From the pole figures, the texture strength before preheating for γ , α , and α' phases are 1.5 m.r.d., 1.2 m.r.d., and 1.9 m.r.d., respectively. This result shows that, in the process of making steel through the casting process, the texture is not too strong. Figure 3 shows the recalculation of the pole figures for α' phases using samples following symmetrization from triclinic to orthorhombic. From the recalculated pole figure, although the texture strength is not too strong, it has a crystallite orientation of $\{001\} \langle 110 \rangle$.

The texture of the γ -phase has a range of texture strength between 0.525 m.r.d. and 1.542 m.r.d. From the results of the recalculated pole figures using triclinic to orthorhombic symmetry, the crystal orientation is found to be a cubic type $\{001\} \langle 100 \rangle$. Figure 4 show recalculated pole figures of γ -phase with triclinic to orthorhombic symmetrization.

In the α -phase, diffraction from the peak 200 is attenuated. Using the (110) and (211) Bragg peaks, from Figure 5, the value of texture strength is between 0.9 to 1.2 m.r.d. The value of the texture strength indicates that there is hardly any texture in the α -phase.

Texture after preheating. Heating at a temperature of $250 \text{ }^\circ\text{C} \pm 10 \text{ }^\circ\text{C}$, shows just the γ - phase, with the other phase not being visible. The apparent texture strength of the pole figure ranges from a minimum of 0.442 to a maximum of 2.398 m.r.d., which is different compared with the gamma phase before heating with texture strength ranging from 0.525 to 1.542 m.r.d.; thus, heating causes the phase transformation from alpha to gamma. Figure 6 show recalculated pole figures of γ -phase with triclinic to orthorhombic symmetrization after preheating.

The diffraction analysis revealed three phases before preheating. From the texture experiment, the pole figures obtained were analyzed to determine the crystal orientation for each phase. From the pole figures analysis, the martensite phase has orientation $\{001\} \langle 1-10 \rangle$ with Euler angle $(\varphi_1, \Phi, \varphi_2) = (46^\circ, 0^\circ, 0^\circ)$. The austenite phase has a cubic orientation $\{001\} \langle 100 \rangle$, and the ferrite phase has a very low texture, with almost no texture appearing, as indicated by the texture index of less than 1 m.r.d. After preheating, only the austenite phase appears. The austenite phase has the cubic orientation $\{001\} \langle 100 \rangle$ with the Euler angle $(\varphi_1, \Phi, \varphi_2) = (0^\circ, 0^\circ, 0^\circ)$. Because of preheating, a change of orientation from $\{001\} \langle 1-10 \rangle$ to $\{110\} \langle 00-1 \rangle$ occurs. The austenite phase does not change the orientation of the crystallite of $\{001\} \langle 100 \rangle$.

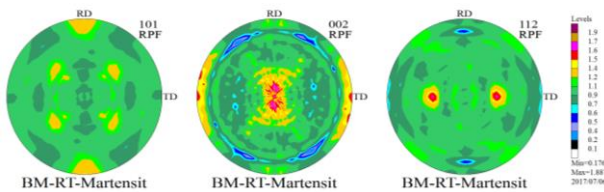


Figure 3. Recalculated Pole Figures of the α' -phase with Triclinic to Orthorhombic Symmetrization

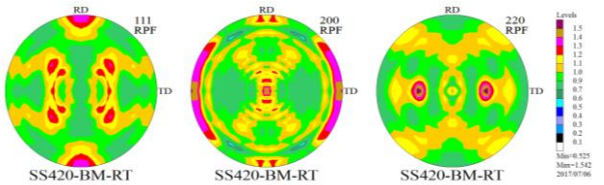


Figure 4. Recalculated Pole Figures of γ -phase with Triclinic to Orthorhombic Symmetrization

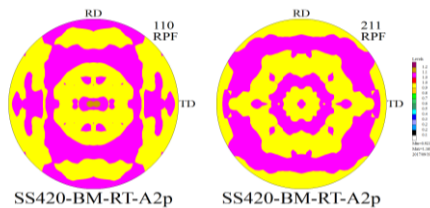


Figure 5. Recalculated Pole Figures of α -phase with Triclinic to Orthorhombic Symmetrization

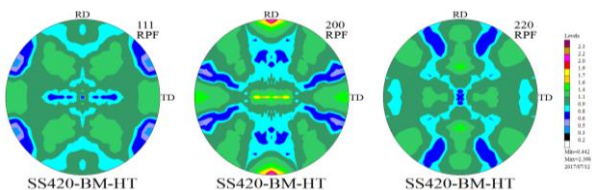


Figure 6. Recalculated Pole Figures of γ -phase with Triclinic to Orthorhombic Symmetrization after preheating

4. Conclusion

From the results of neutron diffraction experiments, before preheating, three phases of martensite, ferrite, and austenite with different weight compositions are found. The largest weight composition is the martensite phase. After preheating at 250°C , the majority phase of martensite is changed to austenite, resulting in a change of the steel properties from nonweldable to weldable.

From the texture analysis, it can be concluded that, before preheating, the crystallite orientation is not too strong. The martensite phase has the crystallite orientation of $\{001\} \langle 110 \rangle$, the austenite phase has the crystallite orientation of $\{001\} \langle 100 \rangle$, and the ferrite phase has almost no texture. After preheating, there is only one phase, namely, the austenite phase with crystal orientation of $\{001\} \langle 100 \rangle$.

Acknowledgement

This research is funded by DIPA PSTBM-BATAN Fiscal Year 2015/2016. The authors wish to thank all parties who have helped us conduct the research study.

References

- [1] Outokumpu, Undergraduate Thesis, Handbook of Stainless Steel, Chalmers University of Technology, Sweden, 2013.
- [2] C. Köse, R. Kaçar, Mater. Des. 64 (2014) 221–226.
- [3] S.A. Jenabali Jahromi, A. Khajeh, B. Mahmoudi, Mater. Des. 34 (2012) 857.
- [4] C.J. Scheuer, R.P. Cardoso, M. Mafra, S.F. Brunatto, Surf. Coatings Technol. 214 (2013) 30.
- [5] L.D. Barlow, J. Mater. Eng. Perform. 21 (2012) 1327.
- [6] J. Zhang *et al.*, Surf. Coatings Technol. 305 (2016) 132.
- [7] S. Yan, E. Compagnon, B. Godin, A.M. Korsunsky, Mater. Today Proc. 2 (2015) S251.
- [8] H.K.D.H. Bhadeshia, Mater. Sci. Metall. 16 (2002) 1.
- [9] F.M. Castro Cerda, C. Goulas, I. Sabirov, L.A.I. Kestens, R.H. Petrov, Mater. Charact. 130 (2017) 188.
- [10] L. Beres, A. Balogh, W. Irmer, Weld. J. (2001) 191.
- [11] R.B. Sanchez-cabrera, Rubio-Gonzalez, Ruiz-Vela, Mater. Sci. Eng. A. 452–453 (2007) 235.
- [12] Z. M. Shi *et al.*, Mater. Charact. 107 (2015) 29.
- [13] M. Shirdel, H. Mirzadeh, M.H. Parsa, Mater. Charact. 103 (2015) 150.
- [14] F. Christien, M.T.F. Telling, K.S. Knight, Mater. Charact. 82 (2013) 50.
- [15] F. Scandella *et al.*, Procedia Eng. 66 (2013) 108.